

Review

Comparative Aspects of Ricin Toxicity by Inhalation

Alexander Stoll *, Daniel P. Shenton, A. Christopher Green and Jane L. Holley

Defence Science and Technology Laboratory, Salisbury SP4 0JQ, UK; dpshenton@dstl.gov.uk (D.P.S.);
acgreen@dstl.gov.uk (A.C.G.); jlholley@dstl.gov.uk (J.L.H.)

* Correspondence: astoll@dstl.gov.uk

Abstract: The pathogenesis of ricin toxicity following inhalation has been investigated in many animal models, including the non-human primate (predominantly the rhesus macaque), pig, rabbit and rodent. The toxicity and associated pathology described in animal models are broadly similar, but variation appears to exist. This paper reviews the published literature and some of our own unpublished data and describes some of the possible reasons for this variation. Methodological variation is evident, including method of exposure, breathing parameters during exposure, aerosol characteristics, sampling protocols, ricin cultivar, purity and challenge dose and study duration. The model species and strain used represent other significant sources of variation, including differences in macro- and microscopic anatomy, cell biology and function, and immunology. Chronic pathology of ricin toxicity by inhalation, associated with sublethal challenge or lethal challenge and treatment with medical countermeasures, has received less attention in the literature. Fibrosis may follow acute lung injury in survivors. There are advantages and disadvantages to the different models of pulmonary fibrosis. To understand their potential clinical significance, these factors need to be considered when choosing a model for chronic ricin toxicity by inhalation, including species and strain susceptibility to fibrosis, time it takes for fibrosis to develop, the nature of the fibrosis (e.g., self-limiting, progressive, persistent or resolving) and ensuring that the analysis truly represents fibrosis. Understanding the variables and comparative aspects of acute and chronic ricin toxicity by inhalation is important to enable meaningful comparison of results from different studies, and for the investigation of medical countermeasures.



Citation: Stoll, A.; Shenton, D.P.; Green, A.C.; Holley, J.L. Comparative Aspects of Ricin Toxicity by Inhalation. *Toxins* **2023**, *15*, 281. <https://doi.org/10.3390/toxins15040281>

Received: 20 March 2023

Revised: 30 March 2023

Accepted: 4 April 2023

Published: 13 April 2023

Keywords: ricin; inhalation; comparative anatomy; comparative pathology

Key Contribution: Understanding the variables and comparative aspects of acute and chronic ricin toxicity by inhalation is important to enable meaningful comparison of results from different studies and for the investigation of medical countermeasures. This paper presents factors potentially contributing to variation between studies, including methodological, species and strain factors. Chronic pathology, from sublethal exposure or lethal exposures with countermeasures, has received less attention in the literature; therefore, factors to consider in this area are discussed.



Copyright: © Crown copyright (2023), Dstl. This material is licensed under the terms of the Open Government Licence except where otherwise stated. To view this licence, visit <http://www.nationalarchives.gov.uk/doc/open-government-licence/version/3> or write to the Information Policy Team, The National Archives, Kew, London TW9 4DU, or email: psi@nationalarchives.gov.uk.

1. Introduction

1.1. Ricin Toxin and Mechanism of Action

Ricin is a type 2 ribosome-inactivating protein (RIP) from the seeds of the castor oil plant (*Ricinus communis*) [1]. Type 1 RIPs are a single-A-chain entity, with little toxicity to animal cells [1,2]. Type 2 RIPs exist as dimeric protein toxins with an A chain with catalytic properties and a B chain with cell-binding properties [2]. The uptake of ricin into cells is undertaken via endocytosis, in which ricin binds to cell surface oligosaccharides [1] or mannose receptors [3,4]. There are multiple, sometimes conflicting, reports on the expression of mannose receptors in different cell populations [3,5–7] (see Section 1.3 for more details). Once in the cytosol, depurination of a single adenine residue (located in the sarcin-ricin loop) of ribosomal 28S RNA leads to arrest of mRNA translation by preventing binding of elongation factor-2 to the ribosome [2]. It is suggested (data are lacking), that

~2000 ribosomes are inactivated per minute by one ricin molecule [8]. Concomitantly, an initiation of events leading to an inflammatory response begins [6,9]. Actions of RIPs beyond ribosome inactivation are due to broader enzymatic activity, such as the release of adenine from DNA and other polynucleotides; thus, inhibition of protein synthesis may be just one mechanism of RIP-mediated cell death [10]. Sequelae include cell death (e.g., necroptosis, apoptosis) [10], changes in mRNA expression [11], ribotoxic stress response and nuclear factor kappa B pathway activation, NALP3 inflammasome-mediated interleukin 1B activation, release of pro-inflammatory mediators [9,12] and oxidative stress, including exacerbation of tissue damage by reactive oxygen species [13].

1.2. Respiratory Tract Deposition, Distribution and Clearance of Inhaled Ricin

Tissue deposition, clearance and distribution vary between method of exposure, species and dose. A greater deposited dose has been reported to be associated with slower clearance, and increased lung damage occurs at higher ricin doses [14].

In a low-dose (a dose which kills 20–30% of the study population; LD₂₀-LD₃₀) intratracheal instillation model, ricin was detected using ELISA in the lung wash of Porton Wistar rats associated with the fluid fraction, and to a small extent the cell fraction, at 24 h after instillation, but was no longer detectable in lung wash at 48 h. Ricin was, however, still detectable within lung tissue at 48 h [15].

In an experiment exploring nose-only exposure to aerosolised ricin, using Sprague Dawley rats (exposed for 20 or 40 min) and BALB/c mice (exposed for 20 min), ricin clearance was investigated using ELISA of tissue homogenates. Ricin was detected in the nasal turbinates 15 min after exposure, up to 1 h later in mice, and up to 4 h later in rats. Ricin was only detectable in the larynx and trachea of rats exposed for 40 min, clearing with a half-life of 7.62 h [14].

The pulmonary deposition (ng per gram of lung tissue) for similar aerosol concentrations of ricin was 2-fold higher in mice than rats after 20 min of exposure, but the clearance half-lives were comparable [14]. In rats, ricin deposition following 40 min of nose-only exposure was reported to be just over twice the deposition observed following 20 min of exposure [14]. In rats, ricin cleared the lung over a period of 48–72 h; however, animals exposed for 40 min (in this study) did not survive to 72 h. The half-life for ricin clearance appeared to be more than 2.5 times greater in rats in the 40 min exposure group (16 h half-life) than the 20 min exposure group (6 h half-life). The authors suggested this may be due to damage to the lung affecting clearance mechanisms in the higher-exposure group [14]; however, the confidence limits for these data were quite wide.

In a study by another group, a head-only exposure of BALB/c mice to a $3 \times$ LC₅₀ dose ($3 \times$ the concentration time product which will kill 50% of the study population) of aerosolised ricin, ricin was measured via ELISA in fluids and tissues. Ricin was detected within nasal wash 1 h after exposure, but this was found to have diminished significantly when measured 4 h after exposure. This was suggested to be the result of rapid mucociliary clearance. In contrast, ricin was detected in lung lavage fluid for at least 16 h [16].

Bulk flow is the predominant mechanism of ventilation proximal to the terminal bronchioles [17,18]. Particle size should be considered when exploring deposition within the respiratory tract. There are many factors that can affect deposition [19,20], but in general, the dominant mechanism of deposition for large, inhaled particles (>5 µm) is impaction. Medium particles (~1–5 µm) are typically deposited via impaction and sedimentation, whilst for small (<~0.5µm) particles, the dominant mechanism of deposition is diffusion [17,19,20]. Diffusion becomes the dominant mechanism of ventilation in the respiratory zone, due to the massive increase in the cross-sectional area of the airways, reducing airflow. In small airways (e.g., respiratory bronchioles), sedimentation of particles that are too large to diffuse into alveoli occurs due to their “negligibly small diffusion rate” [17].

Ricin particle size within the inhaled airstream and deposition has been investigated [21,22]. In mice exposed to a nose-only aerosol, it was found that with larger ricin particles (5–12 µm), most of the ricin particles were found in the trachea, with ~20% in

the lungs [22]. Smaller particle sizes (1 μm) penetrated more successfully (~60%) into the lungs [21,22]. This resulted in mice receiving supra-lethal doses of the smaller particles dying within 72 h, whilst those receiving larger particles survived [22]. A caveat, however, is that there were a number of factors within the experimental methods that could have affected regional distribution patterns and rates of deposition in this study [22].

Schlesinger's (1985) review of comparative deposition of inhaled aerosols presents a comprehensive exploration of factors, including particle characteristics, respiratory tract anatomy and respiratory parameters (which can be affected by anaesthesia, for example) during exposure [19]. An interesting conclusion, from a comparative aspect, is that humans reach a peak deposition efficiency in the alveolar region at a higher particle size (approx. 2–4 μm) than in experimental animals (approx. 1 μm) [19]. Darquenne (2020) explores deposition in humans, and some of the factors affecting this [20].

1.3. Pathogenesis of Inhaled Ricin Toxicity

Injury associated with inhaled ricin toxicity is mostly confined to the lungs, including marked interstitial pneumonia associated with local pro-inflammatory cytokine release, massive neutrophil infiltration, vascular hyperpermeability, perivascular and alveolar oedema, fibrin deposition, haemorrhage and diffuse airway epithelial necrosis involving all lung lobes [12,23,24]. Eventually, flooding in the lungs leads to respiratory insufficiency and death [12]. These changes in the lungs can be summarised as acute lung injury, with clinical signs resembling acute respiratory distress syndrome [6,12]. Understanding the pathogenesis (and any possible variation between species and strains) is important when investigating targets and timings for potential medical countermeasures.

In mice, it has been demonstrated that it takes 48 h to reach maximum depuration, but there are variable effects on different cell populations [2], due to cell accessibility and cell surface receptors [6]. For example, in a CD-1 mouse model using intratracheal instillation, some cell types bound the toxin early (1–6 h) and some later (18–24 h), and a third group bound the toxin at both the early and later stages after intoxication [6]. This study reported that in the early stages after exposure, pulmonary macrophages (1 h) and dendritic cells (3 h) appear to play an important role in controlling the severity of intoxication, scavenging and degrading ricin via mannose-receptor-mediated uptake, and the cells are eliminated soon after [6], with macrophages contributing to pulmonary inflammation (macrophage responses have been explored in multiple studies) [6,11,14,25–27]. Binding in 'alveolar epithelial cells' (specific binding to type I or II not stated) did not peak until 6 h after ricin exposure, but only type II pneumocytes were eliminated late after intoxication [6]. The late stage includes binding of a second population of dendritic cells (which were proposed not to have mannose receptors; 18 h), B cells (18 h) and pulmonary endothelial cells (24 h), with a third of the endothelial cells eliminated by 72 h after intoxication [6].

The massive recruitment of neutrophils contributes to acute lung injury [11,28]. Endothelial cell dynamics are affected by direct cytotoxicity of ricin, opening of endothelial gaps and leukocyte-mediated injury [29]. The resultant compromise for the air–blood barrier involves both extracellular (e.g. junction protein damage by matrix metalloproteinases) and cellular (epithelial and endothelial) damage and death, resulting in pulmonary oedema [6,28]. If acute intoxication is survived, type II pneumocyte hyperplasia becomes evident 96 h after exposure [30].

2. Animal Models of Ricin Toxicity by Inhalation

There exists one poorly documented report of ricin toxicity (sublethal) by inhalation in humans [31]; therefore, most information comes from animal models. Rhesus macaque [29,32–36], pig [24], rabbit [37], rat [14,38] and mouse [11,14,30,39–42] models of ricin toxicity by inhalation have been used. Administration of ricin into the respiratory tract has been carried out by (i) nose-only [14,37,40,42], (ii) head-only [11,29,32–36,38,41], and (iii) whole-body [30] exposure to an aerosol, or (iv) intratracheal instillation [24,39].

The single report of sublethal ricin toxicity by inhalation in humans described the clinical signs and symptoms in the eight individuals involved, 4 to 8 h after exposure to a sublethal dose. These included fever, nausea, cough, dyspnoea, chest tightness and arthralgias [31]. These are, however, broadly consistent with the signs observed in rhesus macaques (fever, altered breathing rate, dyspnoea) [35,43] and rodents (dyspnoea) [14], and flooding of alveoli and inflammation are consistent across species [21]. The expected clinical signs and symptoms following inhalation of a lethal dose of ricin in humans have been extrapolated and summarised by Griffiths (2011) [21] as a gradual feeling of lassitude, loss of interest in surroundings, loss of appetite, dyspnoea and wheezing and death occurring with anoxic convulsions.

2.1. Toxicity of Inhaled Ricin

The dose which kills 50% of a study population (LD_{50}), for ricin toxicity by inhalation in some of these animal models is summarised in Table 1. Although it is conventional in inhalation toxicology to express lethal challenges as the concentration time product which kills 50% of the study population (LCt_{50}) [21], the lethal challenges are listed as median LD_{50} to allow easy comparison with other routes of exposure to ricin. The LD_{50} for an aerosol exposure is calculated from the LCt_{50} and uses the inhaled minute volume as determined using either a literature-derived estimate (most common) or measurement prior to or during the exposure using plethysmography (less common).

There are multiple potential sources of variation in toxicity. *Ricinus communis* cultivars exhibit varying morphology of the plant and seeds, and isotoxins of ricin have been shown to have differing chemical properties, which are thought to affect toxicity [1,21,23,44]. Whether the ricin preparation is a crude or pure extraction is also important [1]. The animal models described include a number of methods of exposure of the respiratory tract to the ricin toxin, introducing variability. These include head-only, nose/muzzle-only and whole-body exposure to an aerosol of ricin, or intratracheal instillation of ricin toxin. Assumptions used to calculate dose (total or retained estimate), aerosol characteristics including particle size delivered and respiratory parameters and animal species and strain differences may also contribute to variation [1,14,19,22].

Table 1. LD_{50} cited for toxicity of ricin by inhalation.

Strain	Exposure	LD_{50} ($\mu\text{g}/\text{kg}$)	Reference
Mouse			
C57/BL6	Intratracheal instillation	10 (estimated)	[39]
BALB/c	Whole body	14.0	[30]
BALB/c	Whole body	11.2	Cited by [1]
BALB/c	Not stated	1.0–10.0 (varying particle sizes)	[22]
BALB/c	Head only	10.4	[41]
BALB/c	Nose only	0.58 (inconsistent aerosol concentration)	[14]
Swiss Webster	Nose only	4.0	[40]
BXSB	Not stated	2.8	Cited by [1]
CD-1	Nose only	>3.0	[42]

Table 1. Cont.

Strain	Exposure	LD ₅₀ (µg/kg)	Reference
Rat			
Porton Wistar	Head only	3.7 (var. <i>Hale Queen</i>)	[1,45]
Porton Wistar	Head only	9.8 (var. <i>Zanzibariensis</i>)	[1,45]
Sprague Dawley	Nose only	0.24 (assuming 20% deposition and an assumed minute volume)	[14]
Rabbit			
New Zealand White	Muzzle only	3.0	[37]
Pig			
Yorkshire x Landrace	Intratracheal instillation	LD ₅₀ not stated. A 1 µg/kg does resulted in no signs, 3 µg/kg resulted in death of all animals.	[24]
Non-human primates			
Rhesus macaque	Head only	15.0	Cited by [1]
Rhesus macaque	Head only	15.5	Dstl unpublished data
Rhesus macaque	Head only	5.8	[29]
African green monkey	Not stated	5.8	Cited by [1]

2.2. Comparative Anatomy Relevant to Ricin Toxicity by Inhalation

Anatomical differences in the respiratory tract between species alter their ability to filter larger airborne particulates, the penetration of inhaled material through the respiratory tract, cellular composition ('targets' for ricin toxin), functional response to xenobiotics and clearance [1]. The immune response between species is also a source of variability [46,47]. Table 2 summarises the broad anatomical differences between the human, non-human primate, pig and rodents (although there may also be strain variability within a species). The cell types that line the respiratory tract vary in type and distribution between species, and there are some differences between the biology of the same cell types in different species.

Briefly, the cell types and their functions are as follows. Ciliated cells function to move the mucous blanket and particulate matter up the airways. Club cells have multiple functions, including immune modulation, xenobiotic metabolism (possess cytochrome P-450-dependent mono-oxygenase system) and synthesis of components of the mucociliary blanket, and serve as a progenitor of ciliated cells [48,49]. Goblet cells secrete mucins, and serous cells produce secretions containing enzymes (bactericidal, for example). Basal cells, found at the base of epithelial cell layers, are stem or progenitor cells for the epithelium [48,49]. Other cells that may be present within the respiratory tract epithelia include neurosecretory or neuroendocrine cells, brush cells (considered sensory receptors) and cells of the immune system [48–50]. The variations in cell types, distribution and biology between species and strains may contribute to the variation in toxicity, lesion distribution and responses to (and windows of opportunity for) medical countermeasures.

Table 2. Comparative features of the respiratory tract of humans, non-human primates, pigs, rats and mice. Information summarised from multiple sources and may vary between strains [1,48–59].

Anatomical Feature	Human	Rhesus Macaque	Pig	Rat	Mouse
Obligate nasal breather	No	No	No	Yes	Yes
Complex turbinates	No	No	Yes	Yes	Yes
Right lung	3 lobes	4 lobes	4 lobes	4 lobes	4 lobes
Left lung	2 lobes	3 lobes	3 lobes	1 lobe	1 lobe
Airway branching	Dichotomous branching		Monopodial branching		
Nasal Cavity					
Vestibule	Stratified squamous epithelium (thinner in rodents).				
	Located between stratified squamous epithelium and respiratory epithelium.				
Nasal transitional epithelium	Thick, stratified, few ciliated, epithelium, including occasional goblet cells.	Non-ciliated columnar epithelium.		Thin, pseudostratified, non-ciliated, basal, columnar and cuboidal epithelium with scattered ciliated cells. Contains abundant smooth endoplasmic reticulum (P450) for xenometabolism.	
Nasal respiratory epithelium	Covers most of the nasal cavity of primates. Pseudostratified, ciliated, columnar epithelium. Gradual increase in goblet cell density anterior to posterior. Varies according to intranasal location.	Pseudostratified, ciliated, columnar epithelium with goblet cells appearing by the nasopharynx. Thick basal lamina.		<50% nasal cavity. Ciliated, goblet and basal cells. Lesser numbers of non-ciliated cells, chemoreceptor and brush cells. P450 for xenometabolism. Varies according to intranasal location.	
Nasal olfactory epithelium	<3% of nasal cavity of human. Lines the medial superior vertical lamellae of the superior turbinates and the corresponding superior septum. There is, however, considerable variability among individuals.	~5% of nasal cavity in monkeys. Present on dorsal parts of the nasal septum, medial turbinates, and lateral wall.	Present on caudodorsal, portion of nasal cavity, dorsal nasal meatus, nasal septum and ethmoturbinates.	~50% of nasal cavity of rats and mice. P450 for xenometabolism. Lines upper caudal third of the septum, dorsal meatus, caudolateral wall and dorsal aspects of ethmoturbinates.	
	Pseudostratified, columnar, neuroepithelium. 3 cell types: Olfactory sensory neurons, basal cells and sustentacular cells.				
Anatomical feature	Human	Rhesus macaque	Pig	Rat	Mouse
Lateral nasal gland	Absent	Secretory products drain into nasal vestibule. Major site of synthesis and secretion of odorant-binding proteins. Synthesises large amounts of immunoglobulin A. High metabolic capacity, potential target for secondary metabolites of inhaled or ingested xenobiotics.			
Trachea					
Ciliated cells	49%	33%	Present	32–41%	39%
Club cells	0%	0%	Not reported	0%	49%
Goblet cells	9%	17%	Present	<1–2%	<1%
Serous cells	0%	0%	Not quantified	27–42%	<1%
Basal cells	33%	42%	Not quantified	13–27%	10%
Other	9%	8%	Not quantified	0–13%	1%

Table 2. Cont.

Anatomical Feature	Human	Rhesus Macaque	Pig	Rat	Mouse
Proximal intrapulmonary airways					
Ciliated cells	37%	44%	Present	35%	28–36%
Club cells	0%	0%	Not reported	0%	59–61%
Goblet cells	10%	15%	Present	<1%	<1%
Serous cells	3%	0%	Not quantified	21%	<1%
Basal cells	32%	32%	Not quantified	27%	<1%
Other	18%	8%	Not quantified	16%	2–14%
Terminal bronchioles					
Ciliated cells	52%	50%	Proximally only	55%	20–40%
Club cells	0%	0%	Present	37%/40–65%	60–80%
Goblet cells	Present	20%	Absent	0%	0%
Serous cells	35%	Not quantified	Not quantified	0%	0%
Basal cells	<1%	10%	Not quantified	0–<1%	<1%
Other	13%	Not quantified	Not quantified	8%	0%
Respiratory bronchioles					
Ciliated cells	Present	<10%	Respiratory bronchioles often lacking (further characterisation of variation between strains required).		
Club cells	Present	>90%			
Goblet cells	Present	Present			
Serous cells	Present	Present			
Basal cells	Present	Present			
Alveoli					
Size (mean linear intercept)	210 μm	200 μm	133 μm	100 μm	80 μm
Blood–gas barrier thickness	0.62 μm	0.65 μm	0.2–0.6 μm	Not reported	0.32 μm
Airway mucus					
Mucus and mucin glycoproteins	Species differences and significances to be determined. Pigs have numerous submucosal glands in the trachea and bronchi.				

2.3. Comparative Pathology of Acute Ricin Toxicity by Inhalation

The pathological changes associated with acute ricin toxicity are broadly similar between species and are detailed for each species at each level of the respiratory tract below. A notable difference includes the rarity of lesions reported (when included in necropsy protocols) in the nasal cavity of the rhesus macaque, compared to the rodent models (see descriptions for each tissue below for more detail). There has been observation of inflammation of the nasal septum of the rhesus macaque in a chronic study [29]. One speculated cause could be the differences in the biotransformation capability of the cell populations (see Table 2) present in the nasal mucosa [60]. The inclusion of nasal cavity samples in necropsy protocols could be considered in future experiments to investigate this further. Another difference is the occurrence of pulmonary oedema in BALB/c mouse models of acute ricin toxicity by inhalation, where it may be present [11] in mice exposed to low doses of ricin, or absent following exposure to high doses [14]. Differences highlight the requirement to select the appropriate species and strain for the model objectives as well as challenge dose.

Table 3 is a summary of the models cited (acute and chronic pathology), comparing the method of exposure, dose, end point(s) and if a countermeasure was used.

Table 3. Animal model comparisons; summarising the animal models cited.

Reference	Countermeasure	Route of Entry	Dose	End Point(s)
Rhesus macaque				
[32]	None	Inhalation, head only	27.2–41.8 µg/kg	48 h
Dstl unpublished data	Antitoxin	Inhalation, head only	3 × LD ₅₀	11–14, 90 days
[29]	None	Inhalation, head only	13.2–27.3 µg/kg (lethal) 1.9–5.2 µg/kg (sublethal)	30–48 h, 11 days
[33]	None	Inhalation, head only	9.4–38.5 µg/kg (lethal) ~3 µg/kg (sublethal)	25–52 h, 11–20 days
[34]	Vaccination	Inhalation, head only	12–38 µg/kg	14 days
[35,36]	Antitoxin (monoclonal antibody) 4 or 12 h after exposure	Inhalation, head only	3 × LD ₅₀	14 days
Pig				
[24]	None	Intratracheal instillation	3 µg/kg	30–70 h
Rabbit				
[37]	Vaccination	Inhalation, muzzle only	10–30 × LD ₅₀	95 days
[61]	None or topical wash	Topical ocular	1 µg–100µg	24 h, 7 days
Rat (Porton strain)				
Dstl unpublished data	None	Inhalation, head only	Various	21 days
[38]	None	Inhalation	11.21 mg/min/m ³ (LC _{t30})	48 h
Reference	Countermeasure	Route of entry	Dose	End point(s)
Rat (Sprague Dawley)				
[14]	None	Inhalation, nose only	0.12 µg/L	7 days
Mouse (BALB/c)				
[14]	None	Inhalation, nose only	0.01 µg/L	7 days
[30]	None	Inhalation, whole-body exposure	14 µg/kg	196 h
[11]	None	Inhalation, head only	11.08 µg/kg	96 h
Dstl unpublished data	None	Inhalation, head only	3.5 or 5.2 mg/min/m ³	96 days
Mouse (C57Bl/6)				
[39]	None	Intratracheal instillation	20, 50 and 200 µg/kg	48 h, 4 weeks
Swiss Webster				
[40]	Vaccination	Inhalation, nose only	1–16 µg/kg (inhalation)	14 days

2.3.1. Nasal Cavity

Rhesus Macaque

Frothy fluid may flow from the nares at death [32]. In studies examining the nasal cavity, no acute lesions were reported [29,34]. Acute, necrotising inflammation has been observed in a single animal exposed to aerosolised ricin (Dstl unpublished data).

Rabbit (New Zealand White)

The pharyngeal mucosa may appear reddened with brown mucoid material on the nasal or ethmoid turbinates, reported on the superior and more caudal portions [37]. Histopathological changes include heterophilic inflammation and necrosis of respiratory epithelial cells of the nasal cavity and turbinates [37].

Rat (Sprague Dawley)

Lesions are described primarily at the level of nasal turbinate 1, with minimal-to-mild mucous cell hyperplasia and hypertrophy, not associated with dose [14].

Mouse (BALB/c)

Lesions are described primarily at the level of nasal turbinate 1, presenting as minimal inflammation [14].

2.3.2. Larynx and Trachea

Rhesus Macaque

Frothy fluid may extend from the lungs into the conducting airways. Animals may exhibit mild suppurative laryngitis and/or tracheitis, epithelial degeneration and submucosal oedema, and the tracheal lumen may contain fibrin, cellular debris and extravasated erythrocytes [29,32,34]. Tracheal inflammation has been reported as diffuse, acute inflammation on a background of chronic inflammation [32], and in two animals as focal and ulcerative (Dstl unpublished data).

Rabbit (New Zealand White)

The laryngeal and tracheal mucosa may be reddened with froth in the trachea. Histopathological changes described include inflammation and necrosis of epithelial cells of the larynx and trachea [37].

Rat (Porton Wistar)

Necrosis of the epithelia at all levels of the respiratory tract from the larynx to the alveoli has been observed. The trachea may be oedematous and contain sloughed necrotic material and haemorrhage (Dstl unpublished data).

Rat (Sprague Dawley)

Dose-dependent mild to moderate mucosal and submucosal inflammation has been reported in the larynx. Mucosal epithelial apoptosis and necrosis were observed in rats dying from exposure. Mucosal epithelial degeneration (dose-dependent) and squamous metaplasia occurred [14]. Epithelial inflammation, cell death and degeneration also developed in the tracheas of rats dying following ricin inhalation, and the severity was described as dose-dependent. In survivors, half of the animals had residual inflammation, whilst all of the survivors exhibited epithelial degeneration [14].

Mouse (BALB/c)

Dose-dependent minimal to mild mucosal and submucosal inflammation has been reported in the larynx. Mucosal epithelial apoptosis and necrosis were observed in mice dying from exposure [14]. Dose-dependent epithelial inflammation, apoptosis/necrosis and degeneration were observed in the trachea of mice dying following intoxication, but were rare in survivors [14].

2.3.3. Lungs

Rhesus Macaque

The lungs have been frequently described as appearing wet, heavy, non-collapsed and firm, with prominent rib impressions [29,32–34,36,43]. Multifocal, dark red and mottled

areas of varying size have been described on lung lobes, which may ooze frothy fluid from cut surfaces [29,33–36].

Histologically, alveoli, perivascular, peribronchial and peribronchiolar spaces may be flooded by oedema fluid containing abundant fibrin strands, degenerate and viable neutrophils and lesser numbers of lymphocytes, plasma cells and alveolar macrophages, and haemorrhage [29,32–34,43,62]. The bronchiolar epithelium is occasionally described as denuded and necrotic, and both bronchi and bronchioles may contain oedema fluid, cellular debris and fibrin [29,32–36,62].

The alveolar septa may be expanded by fibrin, oedema fluid and inflammatory cells [29,32,34] and haemorrhage [62]. Alveolar spaces can contain oedema fluid mixed with cellular debris and degenerate neutrophils [29,32–35], and eosinophils [36]. The terminal bronchioles, alveolar epithelium and alveolar spaces were the most affected [29,32]. Necrosis may be present, sometimes with partial to complete loss of the alveolar epithelium, architecture and septal integrity [29,32,33].

Vascular necrosis and vessels with reactive endothelia, surrounded by oedema, fibrin and granulocytes leaking into perivascular spaces, may be observed, but large calibre vasculitis has not been reported [29,32,62].

Pig (Yorkshire x Landrace)

In pigs receiving ricin via intratracheal instillation, histological changes were confined to the lungs (the liver, spleen, kidney, adrenal gland, pancreas and heart were also examined). Changes included sequestration of polymorphonuclear cells in the alveolar spaces and interstitium, haemorrhages, interstitial and intra-alveolar oedema, thickening of alveolar septa and formation of hyaline membranes. Neutrophils in the interstitial space and hyaline membranes reached maximal levels at 18 h post-exposure [24].

Rabbit (New Zealand White)

Lungs have been described as mottled red and failed to collapse. Histopathological changes were characterised by fibrinonecrotic pneumonia. Bronchial epithelial hyperplasia, attenuation, loss and necrosis have been observed. Peribronchovascular and interstitial heterophilic inflammation, necrosis and oedema may be accompanied by bronchial and alveolar exudate [37].

Rat (Porton Wistar)

Ultrastructural pathology is described by Brown and White (1997), with changes first appearing by 6 h post-exposure [38]. Histologically, 2 days after exposure, pathological changes to the lung included necrosis and apoptotic deletion of the bronchial and bronchiolar epithelia, with macrophages present in the interstitium, and severe perivascular and intra-alveolar oedema [21].

When comparing histopathology between animals exposed to pure and partially extracted preparation of ricin, the partially extracted ricin caused more tissue damage. This was explained as either being due to underestimation of the ricin concentration or the presence of agglutinin in the crude preparation, exacerbating tissue damage without significantly affecting lethality [1]. The changes in both groups (with more widespread and severe lesions, and a higher lung wet weight/body weight ratio, in the partially extracted group) were early perivascular oedema with widespread perivascular cuffing by acute inflammatory cells. Focal hyperinflation and very focal apoptotic deletion of the respiratory epithelium of the larger airways were also present on day 1 [1]. On day 3, the lesions had progressed in severity, with widespread intra-alveolar oedema associated with acute, destructive alveolitis, and both granulocytes and large mononuclear phagocytic cells contributed to the inflammatory infiltrate. Apoptotic deletion of the respiratory epithelium was still present, with sloughing of this epithelium into the lumen of small airways. Widespread, florid, type II pneumocyte hyperplasia was also present at day 3 [1].

Rat (Sprague Dawley)

Mild to moderate peribronchiolar and perivascular inflammation was a consistent finding in a study using Sprague Dawley rats [14]. In rats receiving a high dose, death occurred within 2 days post-exposure, and minimal to mild vasculitis, haemorrhage and bronchiolar degeneration were present in some animals. Pulmonary oedema was most prominent and occurred with the highest incidence in animals exposed to a middle dose. Parenchymal interstitial inflammation occurred in rats and was inversely proportional to survival time. Mild to moderate alveolar macrophage hyperplasia occurred in rats receiving lower doses of toxin. Type II pneumocyte hyperplasia showed an inverse dose dependence [14].

Mouse (BALB/c)

In the BALB/c branch of the same study in which the Sprague Dawley rats were studied (above), mild to moderate peribronchiolar and perivascular inflammation occurred in all dose groups and at all time points, but pulmonary oedema was not observed in the mice in this study [14]. Minimal to mild vasculitis, haemorrhage and bronchiolar degeneration with apoptosis/necrosis were described 2 to 3 days after exposure in mice receiving a high dose. Parenchymal interstitial inflammation was inversely proportional to survival time. Alveolar macrophage hyperplasia exhibited a similar pattern to interstitial inflammation. Type II pneumocyte hyperplasia showed an inverse dose dependence in mice [14].

Mouse (C57Bl/6)

In mice receiving intratracheal instillation of ricin, 48 h after exposure, there was perivascular and peribronchiolar oedema with infiltration by neutrophils. Disruption and loss of the bronchial epithelium, together with apoptotic bodies, were observed, and haemorrhage, exudate and neutrophils extended into alveoli. Fibrin and fibrinogen were detected in the microvasculature of the alveolar septa [39].

2.3.4. Thoracic Cavity

Rhesus Macaque

The thoracic cavity may contain variable amounts of serous to serosanguineous fluid, which may contain strands to sheets of fibrin coating the visceral pleura [29,32,33], with inflammation observed microscopically [32]. The mediastinum may be oedematous [32,34]. The pericardium may be distended by serous or serosanguineous fluid [32].

Rabbit (New Zealand White)

The thoracic cavity may contain serosanguineous fluid [37].

2.3.5. Lymphoid Tissues

Rhesus Macaque

Bronchus-associated lymphoid tissue (BALT) has been described as depleted [29]. Tracheal, mediastinal and mesenteric lymph nodes of some animals were enlarged (twice the normal size or larger) and oedematous [29,32,33]. Description of loss of corticomedullary and follicular architecture of the tracheobronchial lymph nodes has been reported, with lymphoid depletion and replacement of germinal centres and necrotic cellular debris, together with expansion of these areas and sinuses by degenerate and viable neutrophils, lymphocytes, plasma cells, macrophages, haemosiderophages and free erythrocytes [29,32,34–36]. The inflammation, haemorrhage and necrosis have been reported to extend outside the capsule into surrounding connective and adipose tissue [29,32]. Lymphoid hyperplasia may be observed in the tonsils and mesenteric lymph nodes, with an exhaustion matrix in the follicular centres [29]. Animals may exhibit thymic depletion/atrophy [29]. Within the spleen, there may be lymphoid hyperplasia with an exhaustion matrix in the follicular centres [29].

Rabbit (New Zealand White)

Peripheral and visceral lymph nodes have been reported as reddened and/or enlarged [37]. Mediastinal and mandibular lymph nodes exhibited foci of necrosis, fibrin and heterophilic inflammation within subcapsular sinuses, and draining haemorrhage. The thymus may also appear reddened. Within the spleen, there may be heterophilic and histiocytic inflammation with lymphocytes that appear apoptotic [37].

Rat (Porton Wistar)

Increased apoptotic deletion has been observed within the lymphoid follicles of the spleen (Dstl unpublished data).

Rat (Sprague Dawley)

Thymocyte apoptosis was reported in rats dying from exposure, but was minimal amongst surviving rats. In the spleen, neutrophilic leukocytosis occurred in all rats dying following exposure, but was not present in surviving rats. Minimal to mild lymphocytic and haematopoietic cell apoptosis was present in most rats dying following exposure, and less than half of surviving rats [14].

Mouse (BALB/c)

Thymic atrophy occurred in the mice receiving the highest doses, but was not present in surviving mice. In the spleen, neutrophilic leukocytosis occurred in all mice dying following exposure, and was minimal to mild in surviving mice. Lymphocytic and haematopoietic cell apoptosis occurred in some mice in the highest dose groups but was absent in surviving mice [14].

2.4. Comparative Chronic Pathology of Ricin Toxicity by Inhalation

2.4.1. Nasal Cavity

Rhesus Macaque

Moderate lymphoplasmacytic rhinitis affecting the nasal septum has been reported as an occasional observation, 11 days after exposure [29].

Rabbit (New Zealand White, following Vaccination)

Brown mucoid material was present on the nasal or ethmoid turbinates of most animals, predominantly on the superior and more caudal portions. The pharyngeal mucosa was reddened in most animals [37]. Microscopically, lymphoplasmacytic and heterophilic inflammation but no necrosis of respiratory epithelial cells was observed. The non-specific immune response was suggested to be either a mechanism for resolving lesions after ricin exposure or an unidentified inhaled irritant or hypersensitivity reaction [37].

2.4.2. Larynx and Trachea

Rhesus Macaque

Mild lymphoplasmacytic infiltration has been observed in the tracheal mucosa and submucosa 11 days after exposure [29]. Mild chronic inflammation of the trachea has been observed in one of three animals, 90 days after exposure to 3 x LD₅₀ aerosolised ricin and treatment with antitoxin (Dstl unpublished data).

Rabbit (New Zealand White, following Vaccination)

The laryngeal and tracheal mucosa was reddened in most animals. Froth was present in the trachea infrequently. Histopathological changes included inflammation of the larynx and trachea, but no necrosis [37].

2.4.3. Lungs

Rhesus Macaque

Variation in the appearance of lung tissue 11 days after exposure has been described [29]. Changes may include rib impressions, multifocal to coalescing or diffuse mottled discoloration, firm areas, rubbery texture, collapse and increased lung weight [29].

Histological changes 11 days after exposure were more similar between animals [29]. In animals who survived lethal doses, with the administration of an antitoxin, the histopathological changes in the lungs resembled those of animals who received a sublethal dose of ricin [33–35].

Low-grade [34] to prominent [29] type II pneumocyte hyperplasia has been noted multifocally, and small lakes of oedema and dilated lymphatics may remain 11 days after exposure [29]. The smooth muscle around larger airways may appear hyperplastic 11 days after exposure [29]. Lung damage may still be significant 21 days after exposure, with fibrinous accumulation present in the lungs [43].

Animals culled at 14, 20 or 21 days exhibit chronic inflammation and fibrosis proximal to the respiratory bronchioles [33–36]. Bhaskaran et al. (2014) [29] suggest the degree of fibrosis and associated changes are related to the inhaled dose of ricin. Fibrosis is often described as being most prominent around terminal/respiratory bronchioles and the interstitium surrounding larger blood vessels. Fibrosis has been described as extending into the alveolar septa and expanding the interstitium, where it replaces normal alveolar architecture and traps cellular and granulocyte debris [29,34]. In one study, no significant difference was observed between the amount of fibrosis between the lobes of an individual animal or the same lobes between different animals, 11 days after exposure [29]. Fibrosis may still be extensive 21 days after exposure [43].

Admixed within the areas of fibrosis, variable populations of mixed inflammatory cells, mainly lymphocytes and histiocytes with lesser numbers of plasma cells and eosinophils, are reported [29,34]. Surrounding the areas of fibrosis and within the alveolar spaces were large numbers of foamy macrophages, lesser numbers of multinucleated giant cells, degenerate granulocytes and occasional aggregates of lymphocytes, plasma cells and siderophages 11 days after exposure [29]. Macrophage populations have been characterised 20 days after exposure to sublethal doses of inhaled ricin [33]. Confocal microscopy revealed that the majority of intra-alveolar, large and foamy macrophages were the anti-inflammatory M2 subtype (CD68 and CD163 expression). Interstitial macrophages, however, expressed MAC387, a marker believed to be associated with early stages of tissue infiltration [33].

After 34 days, there may be mild pulmonary fibrosis at the level of the respiratory bronchioles. Some resolving pathological changes were observed 90 days after exposure. Changes included widely separated foci of minimal chronic inflammation (one of three animals) and minimal fibrosis (two of three animals) near terminal bronchioles in animals exposed to $3 \times LD_{50}$ aerosolised ricin and treatment with an antitoxin (Dstl unpublished data).

Rabbit (New Zealand White, following Vaccination)

The lungs were mottled red in some of the animals 2 weeks and 12 weeks after exposure, and portions of lung lobes did not collapse in some animals [37]. Microscopic examination after 2 weeks included mild to marked inflammation, with heterophils, lymphocytes, plasma cells and macrophages expanding the peribronchiolar, peribronchial and perivascular connective tissue, and extending into the adjacent interstitium. There was occasional type II pneumocyte hyperplasia and fibrosis, and macrophages and multinucleated giant cells were present in bronchioles. Bronchiolitis obliterans was also present, multifocally [37].

After 12 weeks, microscopic examination revealed minimal to mild inflammation in a similar pattern (but rarely extending into the adjacent interstitium), with low numbers of lymphocytes and fewer plasma cells, macrophages and heterophils. There were low

numbers of alveolar histiocytes, rare multinucleated giant cells and minimal to mild bronchiolitis obliterans in a few animals [37].

Rat (Porton Wistar)

At 3 days after exposure, there was diffuse, marked, alveolar oedema, established acute alveolitis, severe capillary congestion and infiltration of the interstitium by large activated macrophages. Focal areas of type II pneumocyte hyperplasia were present. The large airways continued to exhibit epithelial necrosis with early evidence of regeneration. At 4 days after exposure, the pulmonary oedema was resolving and pulmonary consolidation was evident, with small lymphocytes, activated macrophages and marked type II pneumocyte hyperplasia. The larger airways were completely re-epithelialised and free of oedema fluid [21].

At 7 days, areas of near-normal lung appeared between islands of consolidation and the aforementioned changes [21]. The changes became dominated by widespread nodular consolidation of the lung parenchyma, with foci of collapsed alveoli lined by hyperplastic type II pneumocytes, infiltration by large activated macrophages and, sometimes, extravasated erythrocytes [1]. Some alveoli may still contain oedema fluid [1]. At 14 days, all animals appeared near normal with focal areas of intra-alveolar foamy macrophage infiltration [21].

Rat (Sprague Dawley)

Interstitial fibrosis was present in rats surviving 7 days [14].

Mouse (BALB/c)

In one study, interstitial fibrosis was not observed in mice surviving 7 days [14].

With sublethal doses, minimal alveolar congestion may be present in the first 24 h after exposure [11]. At 48 to 96 h, there may also be foci of necrosis in bronchial and bronchiolar epithelia, alveolar oedema and acute inflammation. Bronchial epithelial hyperplasia may be observed at 96 h [11]. In mice receiving $1 \times LD_{50}$, survivors exhibited type II pneumocyte hyperplasia, pulmonary oedema, bronchiolar epithelial reactivity, peribronchial-vascular fibroplasia and neutrophilic infiltration at 96 h post-exposure [30].

In mice exposed to sublethal doses of inhaled ricin, development of acute inflammation and damage within the lungs developed over days 1 to 7, and gradually subsided over days 21 to 96. Residual pathological changes at day 96 in most animals included areas of peribronchial and perivascular inflammation, alveolar walls thickened by histiocytic infiltration, congestion, alveolar oedema and alveolar haemorrhages (Dstl unpublished data).

Increased connective tissue (possible fibrosis, but not characterised further) has been observed at 96 days in peribronchiolar and perivascular regions in some animals, and some statistically significant lung volume changes were observed (Dstl unpublished data). Further work is required to verify if this is true fibrosis and the significance of these findings in this strain (see Section 2.5 for comparative aspects of animal models of pulmonary fibrosis).

Mouse (C57BL/6)

After 48 h, following intratracheal instillation of a sublethal dose, there was parenchymal accumulation of inflammatory cells, of which most were neutrophils. ERK, JNK and nuclear factor kappa B and Caspase 3 reactivity were also increased, as detected by immunohistochemistry. In the sublethal exposure group, there was no haemorrhage, nor fibrin deposition, in pulmonary tissues, compared to the lethal group in this study [39]. Examination of tissue sections taken from the mice receiving a lethal dose, at higher magnification, revealed that fibrin was localised primarily within the microvasculature of the alveolar septa (proposed to be the initiation of thrombosis, due to leukocyte–endothelial interaction). After 4 weeks, there was no residual leukocyte infiltration in the sublethal group; however, there was interstitial deposition of collagen (fibrosis) [39].

Mouse (Swiss Webster) (Vaccinated)

Aerosol challenge in vaccinated mice, at varying vaccine doses, revealed the following histopathological changes [40]. A total of 21 days after the challenge, there was mild to significant bronchiolar epithelial hyperplasia and smooth muscle hyperplasia of small arteries. In animals surviving to 50 days, changes were limited to mild epithelial hyperplasia, pseudopolyps within scattered bronchioles, mild smooth muscle hyperplasia of arterioles, minimal lymphoid hyperplasia in bronchial lymphoid tissues and no prominent perivascular inflammation. Multifocal type II pneumocyte hyperplasia was observed in one animal [40].

2.4.4. Thoracic Cavity

Rhesus Macaque

Minimal, focal areas of chronic inflammation were observed on the pleura, 90 days after exposure, in one of three animals exposed to $3 \times LD_{50}$ aerosolised ricin and treated with an antitoxin (Dstl unpublished data).

2.4.5. Lymphoid Tissues

Rhesus Macaque

Lymph nodes may be enlarged by two to five times their normal size 11 days after exposure [29]. Histologically, 11 to 14 days after exposure, lymph nodes, including tracheobronchial, mesenteric, inguinal and axillary lymph nodes, appeared reactive, with large lymphoid follicles but a decreased number of lymphocytes in the germinal centres (exhaustion matrix) [29,34]. The paracortical and medullary regions of the tracheobronchial lymph nodes may have foci of oedema containing foamy macrophages 11 days after exposure [29]. The sinuses and peripheral lymphatics were markedly dilated with numerous pigment (negative for iron)-laden macrophages, and lesser numbers of degenerate neutrophils and eosinophils 11 days after exposure [29]. Within the tonsils, mild to moderate lymphoid hyperplasia was observed 11 days after exposure [29]. After 90 days, generalised, minimal to mild, lymphoid hyperplasia, including BALT, was observed in three of three animals exposed to $3 \times LD_{50}$ aerosolised ricin and treated with an antitoxin (Dstl unpublished data).

The thymus and spleen may exhibit lymphoid hyperplasia 11 days after exposure [29]. The spleen exhibited hyperplasia 90 days after exposure in three of three animals exposed to $3 \times LD_{50}$ aerosolised ricin and an antitoxin (Dstl unpublished data).

Rabbit (New Zealand White, following Vaccination)

Lymph nodes and the thymus were reddened, infrequently, and the lymph nodes exhibited lymphoid hyperplasia but no necrosis [37]. The spleen exhibited lymphoid hyperplasia, heterophilic and histiocytic inflammation, but no necrosis [37].

2.5. Comparative Aspects of Animal Models of Pulmonary Fibrosis

Models to investigate pulmonary fibrosis are an area of interest for those investigating inhaled ricin toxicity, as apparent above. Fibrosis may be a sequel to acute lung injury in survivors (either a sublethal aerosol challenge or lethal aerosol challenge but in the presence of a medical countermeasure). Fibrosis could result in impaired lung elasticity and loss of alveolar surface area [63,64], which may affect long-term quality of life, and its prevention is a potential target for medical countermeasures. There are advantages and disadvantages to the different animal models of pulmonary fibrosis, which need to be considered when choosing a model for chronic ricin toxicity by inhalation.

General weaknesses to animal models of pulmonary fibrosis include the relatively long time required for fibrosis to develop; therefore, study design needs to factor in the timeframes in which changes are exhibited. For example, in mouse models of pulmonary fibrosis, the time to develop fibrosis varies by model from 28 days (bleomycin model) to 30 weeks (irradiation models) [63]. Variations exist both between species and between strains. Different mouse strains can be prone to, or exhibit resistance to, fibrosis in different

models [63,64]. For example, BALB/c mice develop limited fibrosis (e.g., bleomycin models) or are resistant to fibrosis (e.g., silica models) in some models, whilst fibrosis develops in others (e.g., fluorescein isothiocyanate models). C57BL/6 mice are irradiation-fibrosis-prone, whilst C3H/HeJ and CBA/J mice are irradiation-fibrosis-resistant [63]. The nature of the fibrosis may also vary; for example, it may be self-limiting, progressive, persistent, or resolve, and this depends on the strain, stimulus and time period [63,64]. Also important in the investigation of pulmonary fibrosis is ensuring that the analysis truly represents fibrosis, by combining biochemical assays and histological evaluation and ideally other techniques, such as lung mechanics and imaging [64].

These variables may explain some of the variation in pathological changes between species and strains seen in the studies of chronic or sublethal exposure in models of ricin survival, with and without countermeasures. As mentioned earlier, amongst other variables, particle size distribution affects ricin deposition, and this may affect distribution of acute lesions. One may also expect, therefore, that the distribution and severity of chronic lesions may be influenced by similar variables, and that this chronic response would be further modified by species- and strain-specific responses to injury. For example, if particle size favours deposition by sedimentation, this might contribute to the distribution of injury and therefore fibrosis observed around respiratory bronchioles in non-human primates (Figure 1).

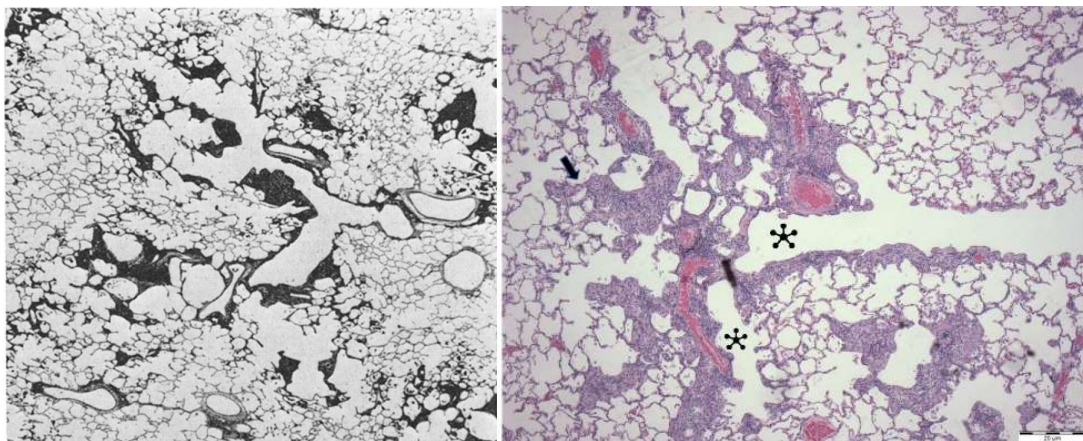


Figure 1. (Left): coal dust deposited around respiratory bronchioles demonstrates the pattern of particle sedimentation in a human [17]. From Heppleston and Leopold (1961) [65], Copyright Elsevier 1961. (Right): The distribution of fibrosis around terminal bronchioles (*) and alveolar septa (arrow) following chronic toxicity to inhaled ricin in the non-human primate (Dstl unpublished data, image taken by J. Novak DVM DACVP).

3. Distant Organ Damage following Ricin Toxicity by Inhalation

3.1. *Rhesus Macaque*

With acute toxicity, adrenal medullary haemorrhage was observed occasionally [29] and there may be cellular degeneration and necrosis within the adrenal cortex [32]. The skin may lose elasticity (dehydration) [32]. The liver, kidney and small intestines may be congested, although with no significant histopathological changes [43]. Our unpublished data also include records of haemorrhage in the omentum and cellular degeneration in the myocardium and kidneys. Minimal chronic myocardial inflammation was reported in one of three animals, 90 days after exposure to $3 \times LD_{50}$ aerosolised ricin and an antitoxin (Dstl unpublished data).

3.2. *Rat (Porton Wistar)*

With acute toxicity, two days after exposure extra-pulmonary organs were reported as unremarkable. Four days after exposure, however, peripheral organs exhibited passive ve-

nous congestion, due to the increased pulmonary vascular resistance caused by significant consolidation [21].

3.3. Mouse Models

In C57BL/6 mice receiving a lethal dose (20 µg/kg) and culled at 48 h, there was infiltration of the kidneys by a mixed population of inflammatory cells into glomerular capillaries, including large numbers of neutrophils. Fibrin and fibrinogen were also deposited within glomerular and interstitial capillaries, as detected by immunohistochemistry, and renal function was affected [39].

Doebler et al. (1995) [42] used radioactive-iodine-labelled ricin (125I-ricin) in a nose-only aerosol exposure (1 µm mass median aerodynamic diameter (MMAD) particles) experiment in CD-1 mice. This revealed the presence of ricin within the gastrointestinal tract, spleen, liver and lung [42]. The presence of ricin in the gastrointestinal tract was assumed to be due to the mice swallowing some of the inhaled toxin [21,42]. The dose calculated to have been swallowed was much lower than that of the inhaled toxin, and the lethal dose by ingestion was much higher, so it was unlikely to have contributed to lethality [21,22].

Benson et al. (2011) [14] detected no ricin in the liver, kidney, stomach, spleen or excreta in any sacrifice or collection time in BALB/c mice exposed via nose-only inhalation, up to 7 days post-exposure. Ricin was not detected in the gastrointestinal tract of another BALB/c mouse study either following head-only exposure to aerosolised ricin [16]. It was suggested that the difference between detection could be due to differences in detection techniques and that Doebler et al. (1995) [42] might be picking up radio-iodine rather than ricin, or that swallowed and denatured ricin was not picked up by the ELISA [21]. Roy et al. (2003) were able to detect low levels of ricin in the stomach of mice exposed to aerosols of ricin using an ELISA [22].

Griffiths et al. (2013) [16] measured ricin in fluids and tissues from BALB/c mice using an ELISA following head-only aerosol exposure to a $3 \times \text{LC}_{50}$ dose. Reliable measurements of ricin were seen in the liver at 24 h after exposure [16]. Although the distribution and detection of ricin in tissues outside the respiratory tract, following inhalational exposure, demonstrates that the toxin can cross the alveoli into the blood, no ricin was detected in blood (plasma or lysed cell pellet) using ELISA or immunochromatography. It was suggested that levels of ricin were below the limit of detection of these methods [16].

3.4. Topical Exposure

In exploring distant organ damage, it is also pertinent to consider other potential consequences of exposure to aerosolised ricin. An individual exposed to an aerosol of ricin could encounter topical (e.g., cutaneous and ocular) contact with the toxin. There is no evidence to suggest that ricin is toxic when applied to the skin [8]. Topical application in mice, with 50 µg of ricin, resulted in no signs of toxicity, due to poor absorption across intact skin [8]. The eyes may also be exposed, and topical administration of ricin to the eye of a rabbit model resulted in dose-dependent pathological changes [61]. The ricin molecule may also be immunogenic and may be associated with hypersensitivity/allergic symptoms (for example, those working in castor bean processing environments) and an IgE-mediated response is proposed for dermatological and ophthalmological signs [31]. This could, however, be complicated by the presence of other allergens in castor bean dust [31].

4. Discussion and Conclusions

Commonly used species in inhalational toxicology studies of ricin include rodents, non-human primates and pigs [1,12,24]. There is consistency in the pathology following ricin toxicity by inhalation between rodents, non-human primates and other species, but there is variation in susceptibility, which can be quite considerable, as well as variation in the location of lesions observed across animal models [1,29]. This is due to, in part, anatomical,

physiological, immunological, cytological and methodological differences. As noted by Bhaskaran et al. (2014) [29], since there are few cases (and no pathology data) of human ricin toxicosis by inhalation to compare, the range of lesions in animal models may prove useful and predictive [1,21,29]. Understanding the comparative aspects of ricin toxicity by inhalation is, therefore, important to aid the development of medical countermeasures.

Approaches to treatment of pulmonary ricin intoxication have been reviewed by Gal et al. (2017) [12]. These include anti-ricin antibodies, interference with the toxin by small-molecule inhibitors and immunomodulatory drugs [12]. These target different mechanisms in the pathogenesis of intoxication, and thus any variation in these mechanisms and pathways between animal models, or introduced by methodological differences, will affect the outcome of their assessment.

Currently, the only post-exposure measure that is effective against pulmonary ricinosis at clinically relevant time points following intoxication in animal models is passive immunisation with anti-ricin-neutralising antibodies [12]. Antibodies are thought to work via a number of mechanisms, including direct inhibition of ricin/uptake as well as effects on intracellular trafficking depending on which part of the ricin molecule the antitoxin binds to.

The assessment of the effectiveness and window of opportunity for different antibody-based therapeutics has potential to provide insight into the early pathogenesis of ricin intoxication following inhalation and also highlights differences between species. For example, an antitoxin that prevents ricin binding to cells may have a shorter window of opportunity than one that disrupts intracellular routing of the toxin. It is difficult to draw comparisons from the literature for ricin inhalation as data involving intoxication via the pulmonary route is limited. Even where pulmonary exposure has been used, it is difficult to make sound comparisons between studies due to differences in their design. For example, the effectiveness for a particular monoclonal antibody, 'PB10' (or variations thereof), has not been demonstrated to be significantly different in the Rhesus macaque [35] or the mouse (BALB/c) [66] following ricin exposure of the lung (although this is hindered by the lack of data between a 4 h and 12 h time point in the Rhesus macaque [35] and beyond 7 h in the mouse model [66]). In addition, the challenge doses and method of administration were significantly different, with a $4 \times LD_{50}$ aerosol challenge used in the non-human primate study and a $10 \times LD_{50}$ intranasal challenge applied in the mouse study. In contrast, a polyclonal F(ab')₂ antibody produced in sheep (which is expected to have a range of activities, including inhibition of binding and effects on intracellular trafficking) demonstrated a window of opportunity of 24 h in mice [41]. This finding is significant as it suggests possible differences in the early stages of ricin intoxication between species.

It is also a significant observation that the window of opportunity in the pig administered a lethal challenge of ricin via intratracheal instillation for an equine-derived antitoxin was (at least) 18 h (85% survival) [67]. The same antitoxin gave ~60% protection when administered 24 h (intravenous or intramuscularly) after an intranasal ricin challenge in CD1 mice [68]. No data for other species have been reported. Some caution is required in direct comparisons as the ricin challenge in studies may differ and the method of administering the toxin may vary between research groups.

The reason for variable windows of opportunity is unknown, but some have speculated causes for these interspecies differences include the volume and composition of mucus within the respiratory tract (as ricin may bind with mucus components, e.g., from porcine submucosal mucus glands of the trachea and bronchi), and/or the cellular composition of the proximal airways (e.g., large numbers of club cells in the mouse trachea) interacting with inhaled ricin.

Another group determined that a polyclonal equine antitoxin was more effective than a monoclonal antibody in mice administered both ricin ($\sim 3 \times LD_{50}$) and therapeutics via the intranasal route, with a survival rate of 100% (polyclonal) versus 50–60% (monoclonal) when administered 18 h after ricin intoxication [69]. This finding demonstrates that focussed studies can elucidate differences in the window of opportunity of antibody therapeutics

and provide data to that may help in the understanding of the mechanism of action of different therapeutics. In this case, the data suggest that different products may intervene at different points in the uptake and intracellular trafficking of ricin. It is likely that a polyclonal antibody therapeutic has multiple targets for intervention (e.g. binding as well as intracellular trafficking of toxin), providing the ability to intervene slightly later than a monoclonal antibody with a single mechanism of action.

The literature demonstrates a delay between exposure to ricin and the morphological changes detectable by routine pathological techniques, such as histopathology. Other indicators may be required, therefore, to elucidate changes in the very early period following exposure and the effects of medical countermeasures, e.g., physiological methods, such as telemetry and pulse oximetry. When histopathology is used, future studies should also include samples of the conducting airways (including the nasal cavity) and lymphoid tissues, as these areas are sometimes neglected.

It is important to consider that differences in anatomy and physiology will affect the choice of exposure method and/or the distribution of toxin [1]. Inhaled aerosol dose determinations and particle deposition are also far more complex than those associated with other administration techniques in animals [70]. The importance of particle size distribution in the aerosol and its relation to deposition in the respiratory tract was outlined earlier. This level of detail is sometimes lacking in published studies of inhaled ricin toxicity using aerosols.

Comparative immunology should also be considered. A comprehensive review of the comparative anatomy of lymphoid tissues in laboratory animals and humans is presented by Haley (2017) [46]. Another review by the same author (Haley 2003) [47] highlights “*data obtained from the evaluation of a single compound in a single species may be insufficient to predict the [immune] response to the same compound in a different species*”.

Understanding and characterising the chronic (sublethal) toxicity of ricin does not feature abundantly in the literature reviewed. A better understanding of this area is required, because if a situation arises where ricin is used as a bioweapon, survivors may have received a low dose, and individuals exposed to higher doses of ricin and treated with a therapeutic may still exhibit some pathological changes and survive to experience chronic changes [29]. In both scenarios, it is important to understand the potential pathological changes, the pathogenesis and their clinical significance, to inform development of treatment strategies and therapeutics [29]. The effects of ricin on primary pulmonary alveolar macrophages were investigated by Guo et al. (2019) [27] providing further understanding of the pathogenic mechanism of inhalational ricin poisoning. Investigating targets associated with macrophage function in lung injury and fibrosis may enable therapeutics that reduce sublethal/chronic effects of ricin. For example, blocking the p38 MAPK signalling pathway reorients macrophage death from pro-inflammatory pyroptosis toward non-inflammatory apoptosis [71].

When exploring sublethal or chronic effects of inhaled ricin intoxication and developing countermeasures, model development requires consideration of the comparative aspects of pulmonary fibrosis and accurate analysis of fibrosis. This could be achieved by combining biochemical assays and histological evaluation and ideally other techniques, such as physiological assessment, lung mechanics and imaging, to ensure changes truly represent fibrosis and detection of any potential clinical significance [63,64].

Finally, many of the comparative factors considered in this paper may apply to the study of the toxicity of other type 2 RIPs by inhalation. Assumptions should not be made, however, due to differences known to exist (abrin, for example [45]) and differences not yet elucidated.

Author Contributions: Conceptualization, A.S. and J.L.H.; writing—original draft preparation, A.S.; writing—review and editing, D.P.S., A.C.G. and J.L.H. All authors have read and agreed to the published version of the manuscript.

Funding: This work was supported by UK Ministry of Defence.

Institutional Review Board Statement: Not applicable. Unpublished data were obtained in accordance with national and institutional regulations.

Data Availability Statement: The data presented in this review are available in the article or cited literature.

Acknowledgments: The authors are grateful to the colleagues, predecessors and collaborators who performed the work cited as ‘Dstl unpublished data’.

Conflicts of Interest: The authors declare no conflict of interest.

References

1. Griffiths, G.D.; Phillips, G.J.; Holley, J. Inhalation toxicology of ricin preparations: Animal models, prophylactic and therapeutic approaches to protection. *Inhal. Toxicol.* **2007**, *19*, 873–887. [[CrossRef](#)] [[PubMed](#)]
2. Falach, R.; Sapoznikov, A.; Gal, Y.; Israeli, O.; Leitner, M.; Seliger, N.; Ehrlich, S.; Kronman, C.; Sabo, T. Quantitative profiling of the in vivo enzymatic activity of ricin reveals disparate depurination of different pulmonary cell types. *Toxicol. Lett.* **2016**, *258*, 11–19. [[CrossRef](#)] [[PubMed](#)]
3. Simmons, B.M.; Stahl, P.D.; Russell, J.H. Mannose receptor-mediated uptake of ricin toxin and ricin A chain by macrophages. Multiple intracellular pathways for a chain translocation. *J. Biol. Chem.* **1986**, *261*, 7912–7920. [[CrossRef](#)] [[PubMed](#)]
4. Newton, D.L.; Wales, R.; Richardson, P.T.; Walbridge, S.; Saxena, S.K.; Ackerman, E.J.; Roberts, L.M.; Lord, J.M.; Youle, R.J. Cell surface and intracellular functions for ricin galactose binding. *J. Biol. Chem.* **1992**, *267*, 11917–11922. [[CrossRef](#)] [[PubMed](#)]
5. Linehan, S.A.; Martínez-Pomares, L.; Stahl, P.D.; Gordon, S. Mannose receptor and its putative ligands in normal murine lymphoid and nonlymphoid organs: In situ expression of mannose receptor by selected macrophages, endothelial cells, perivascular microglia, and mesangial cells, but not dendritic cells. *J. Exp. Med.* **1999**, *189*, 1961–1972. [[CrossRef](#)]
6. Sapoznikov, A.; Falach, R.; Mazor, O.; Alcalay, R.; Gal, Y.; Seliger, N.; Sabo, T.; Kronman, C. Diverse profiles of ricin-cell interactions in the lung following intranasal exposure to ricin. *Toxins* **2015**, *7*, 4817–4831. [[CrossRef](#)]
7. Mooney, B.; Torres-Velez, F.J.; Doering, J.; Ehrbar, D.J.; Mantis, N.J. Sensitivity of Kupffer cells and liver sinusoidal endothelial cells to ricin toxin and ricin toxin-Ab complexes. *J. Leukoc. Biol.* **2019**, *106*, 1161–1176. [[CrossRef](#)]
8. Schep, L.J.; Temple, W.A.; Butt, G.A.; Beasley, M.D. Ricin as a weapon of mass terror—Separating fact from fiction. *Environ. Int.* **2009**, *35*, 1267–1271. [[CrossRef](#)]
9. Lindauer, M.; Wong, J.; Magun, B. Ricin Toxin Activates the NALP3 Inflammasome. *Toxins* **2010**, *2*, 1500–1514. [[CrossRef](#)]
10. Polito, L.; Bortolotti, M.; Battelli, M.G.; Calafato, G.; Bolognesi, A. Ricin: An Ancient Story for a Timeless Plant Toxin. *Toxins* **2019**, *11*, 324. [[CrossRef](#)]
11. David, J.; Wilkinson, L.J.; Griffiths, G.D. Inflammatory gene expression in response to sub-lethal ricin exposure in Balb/c mice. *Toxicology* **2009**, *264*, 119–130. [[CrossRef](#)] [[PubMed](#)]
12. Gal, Y.; Mazor, O.; Falach, R.; Sapoznikov, A.; Kronman, C.; Sabo, T. Treatments for Pulmonary Ricin Intoxication: Current Aspects and Future Prospects. *Toxins* **2017**, *9*, 311. [[CrossRef](#)] [[PubMed](#)]
13. Suntres, Z.E.; Stone, W.L.; Smith, M.G. Ricin-induced toxicity: The role of oxidative stress. *J. Med. Chem. Biol. Radiol. Def.* **2005**, *3*, 1–21.
14. Benson, J.M.; Gomez, A.P.; Wolf, M.L.; Tibbetts, B.M.; March, T.H. The acute toxicity, tissue distribution, and histopathology of inhaled ricin in Sprague Dawley rats and BALB/c mice. *Inhal. Toxicol.* **2011**, *23*, 247–256. [[CrossRef](#)]
15. Cook, D.L.; David, J.; Griffiths, G.D. Retrospective identification of ricin in animal tissues following administration by pulmonary and oral routes. *Toxicology* **2006**, *223*, 61–70. [[CrossRef](#)]
16. Griffiths, G.D.; Knight, S.J.; Holley, J.; Thullier, P. Evaluation by ELISA of Ricin Concentration in Fluids and Tissues after Exposure to Aerosolised Ricin, and Evaluation of an Immunochromatographic Test for Field Diagnosis. *J. Clin. Toxicol.* **2013**, *3*, 1000162. [[CrossRef](#)]
17. West, J.B.; Luks, A.M. *West's Pulmonary Pathophysiology the Essentials*, 9th ed.; Wolters Kluwer: Philadelphia, PA, USA, 2017.
18. West, J.B.; Luks, A.M. *West's Pulmonary Physiology the Essential*, 10th ed.; Wolters Kluwer: Philadelphia, PA, USA, 2016.
19. Schlesinger, R.B. Comparative deposition of inhaled aerosols in experimental animals and humans: A review. *J. Toxicol. Environ. Health* **1985**, *15*, 197–214. [[CrossRef](#)]
20. Darquenne, C. Deposition Mechanisms. *J. Aerosol Med. Pulm. Drug Deliv.* **2020**, *33*, 181–185. [[CrossRef](#)]
21. Griffiths, G.D. Understanding ricin from a defensive viewpoint. *Toxins* **2011**, *3*, 1373–1392. [[CrossRef](#)]
22. Roy, C.J.; Hale, M.; Hartings, J.M.; Pitt, L.; Duniho, S. Impact of inhalation exposure modality and particle size on the respiratory deposition of ricin in BALB/c mice. *Inhal. Toxicol.* **2003**, *15*, 619–638. [[CrossRef](#)]
23. Lord, J.M.; Griffiths, G.D. Ricin: Chemistry, Sources, Exposures, Toxicology and Medical Aspects. In *General, Applied and Systems Toxicology*; Wiley: Hoboken, NJ, USA, 2009.
24. Katalan, S.; Falach, R.; Rosner, A.; Goldvaser, M.; Brosh-Nissimov, T.; Dvir, A.; Mizrachi, A.; Goren, O.; Cohen, B.; Gal, Y.; et al. A novel swine model of ricin-induced acute respiratory distress syndrome. *Dis. Model. Mech.* **2017**, *10*, 173–183. [[CrossRef](#)] [[PubMed](#)]

25. Korcheva, V.; Wong, J.; Lindauer, M.; Jacoby, D.B.; Iordanov, M.S.; Magun, B. Role of apoptotic signaling pathways in regulation of inflammatory responses to ricin in primary murine macrophages. *Mol. Immunol.* **2007**, *44*, 2761–2771. [[CrossRef](#)] [[PubMed](#)]
26. Lindauer, M.L.; Wong, J.; Iwakura, Y.; Magun, B.E. Pulmonary inflammation triggered by ricin toxin requires macrophages and IL-1 signaling. *J. Immunol.* **2009**, *183*, 1419–1426. [[CrossRef](#)] [[PubMed](#)]
27. Guo, Z.; Wang, Z.; Meng, S.; Zhao, Z.; Zhang, C.; Fu, Y.; Li, J.; Nie, X.; Zhang, C.; Liu, L.; et al. Effects of ricin on primary pulmonary alveolar macrophages. *J. Int. Med. Res.* **2019**, *47*, 3763–3777. [[CrossRef](#)] [[PubMed](#)]
28. Sapozhnikov, A.; Gal, Y.; Falach, R.; Sagi, I.; Ehrlich, S.; Lerer, E.; Makovitzki, A.; Alosin, A.; Kronman, C.; Sabo, T. Early disruption of the alveolar-capillary barrier in a ricin-induced ARDS mouse model: Neutrophil-dependent and -independent impairment of junction proteins. *Am. J. Physiol. Lung Cell. Mol. Physiol.* **2019**, *316*, L255–L268. [[CrossRef](#)]
29. Bhaskaran, M.; Didier, P.J.; Sivasubramani, S.K.; Doyle, L.A.; Holley, J.; Roy, C.J. Pathology of lethal and sublethal doses of aerosolized ricin in rhesus macaques. *Toxicol. Pathol.* **2014**, *42*, 573–581. [[CrossRef](#)] [[PubMed](#)]
30. DaSilva, L.; Cote, D.; Roy, C.; Martinez, M.; Duniho, S.; Pitt, M.L.; Downey, T.; Dertzbaugh, M. Pulmonary gene expression profiling of inhaled ricin. *Toxicon* **2003**, *41*, 813–822. [[CrossRef](#)] [[PubMed](#)]
31. Audi, J.; Belson, M.; Patel, M.; Schier, J.; Osterloh, J. Ricin poisoning: A comprehensive review. *JAMA* **2005**, *294*, 2342–2351. [[CrossRef](#)]
32. Wilhelmsen, C.L.; Pitt, M.L. Lesions of acute inhaled lethal ricin intoxication in rhesus monkeys. *Vet. Pathol.* **1996**, *33*, 296–302. [[CrossRef](#)]
33. Pincus, S.H.; Bhaskaran, M.; Brey, R.N., 3rd; Didier, P.J.; Doyle-Meyers, L.A.; Roy, C.J. Clinical and Pathological Findings Associated with Aerosol Exposure of Macaques to Ricin Toxin. *Toxins* **2015**, *7*, 2121–2133. [[CrossRef](#)]
34. Roy, C.J.; Brey, R.N.; Mantis, N.J.; Mapes, K.; Pop, I.V.; Pop, L.M.; Ruback, S.; Killeen, S.Z.; Doyle-Meyers, L.; Vinet-Oliphant, H.S.; et al. Thermostable ricin vaccine protects rhesus macaques against aerosolized ricin: Epitope-specific neutralizing antibodies correlate with protection. *Proc. Natl. Acad. Sci. USA* **2015**, *112*, 3782–3787. [[CrossRef](#)] [[PubMed](#)]
35. Roy, C.; Ehrbar, D.; Bohorova, N.; Bohorov, O.; Kim, D.; Pauly, M.; Whaley, K.; Rong, Y.; Torres-Velez, F.J.; Vitetta, E.S.; et al. A Humanized Monoclonal Antibody against the Enzymatic Subunit of Ricin Toxin Rescues Rhesus macaques from the Lethality of Aerosolized Ricin. *bioRxiv* **2018**, 407817. [[CrossRef](#)]
36. Roy, C.J.; Ehrbar, D.J.; Bohorova, N.; Bohorov, O.; Kim, D.; Pauly, M.; Whaley, K.; Rong, Y.H.; Torres-Velez, F.J.; Vitetta, E.S.; et al. Rescue of rhesus macaques from the lethality of aerosolized ricin toxin. *JCI Insight* **2019**, *4*, 12. [[CrossRef](#)]
37. McLain, D.E.; Lewis, B.S.; Chapman, J.L.; Wannemacher, R.W.; Lindsey, C.Y.; Smith, L.A. Protective effect of two recombinant ricin subunit vaccines in the New Zealand white rabbit subjected to a lethal aerosolized ricin challenge: Survival, immunological response, and histopathological findings. *Toxicol. Sci.* **2012**, *126*, 72–83. [[CrossRef](#)] [[PubMed](#)]
38. Brown, R.F.; White, D.E. Ultrastructure of rat lung following inhalation of ricin aerosol. *Int. J. Exp. Pathol.* **1997**, *78*, 267–276. [[CrossRef](#)]
39. Wong, J.; Korcheva, V.; Jacoby, D.B.; Magun, B. Intrapulmonary delivery of ricin at high dosage triggers a systemic inflammatory response and glomerular damage. *Am. J. Pathol.* **2007**, *170*, 1497–1510. [[CrossRef](#)] [[PubMed](#)]
40. Smallshaw, J.E.; Richardson, J.A.; Vitetta, E.S. RiVax, a recombinant ricin subunit vaccine, protects mice against ricin delivered by gavage or aerosol. *Vaccine* **2007**, *25*, 7459–7469. [[CrossRef](#)]
41. Whitfield, S.J.C.; Griffiths, G.D.; Jenner, D.C.; Gwyther, R.J.; Stahl, F.M.; Cork, L.J.; Holley, J.L.; Green, A.C.; Clark, G.C. Production, Characterisation and Testing of an Ovine Antitoxin against Ricin; Efficacy, Potency and Mechanisms of Action. *Toxins* **2017**, *9*, 329. [[CrossRef](#)]
42. Doebler, J.A.; Wiltshire, N.D.; Mayer, T.W.; Estep, J.E.; Moeller, R.B.; Traub, R.K.; Broomfield, C.A.; Calamaio, C.A.; Thompson, W.L.; Pitt, M.L. The distribution of [¹²⁵I]ricin in mice following aerosol inhalation exposure. *Toxicology* **1995**, *98*, 137–149. [[CrossRef](#)]
43. Roy, C.J.; Song, K.; Sivasubramani, S.K.; Gardner, D.J.; Pincus, S.H. Animal models of ricin toxicosis. *Curr. Top. Microbiol. Immunol.* **2012**, *357*, 243–257.
44. Worbs, S.; Köhler, K.; Pauly, D.; Avondet, M.A.; Schaer, M.; Dorner, M.B.; Dorner, B.G. Ricinus communis intoxications in human and veterinary medicine—a summary of real cases. *Toxins* **2011**, *3*, 1332–1372. [[CrossRef](#)]
45. Griffiths, G.D.; Rice, P.; Allenby, A.C.; Bailey, S.C.; Upshall, D.G. Inhalation toxicology and histopathology of ricin and abrin toxins. *Inhal. Toxicol.* **1995**, *7*, 269–288. [[CrossRef](#)]
46. Haley, P.J. The lymphoid system: A review of species differences. *J. Toxicol. Pathol.* **2017**, *30*, 111–123. [[CrossRef](#)] [[PubMed](#)]
47. Haley, P.J. Species differences in the structure and function of the immune system. *Toxicology* **2003**, *188*, 49–71. [[CrossRef](#)] [[PubMed](#)]
48. Herbert, R.A.; Janarshan, K.S.; Pandiri, A.R.; Cesta, M.F.; Miller, R.A. Nose, larynx, and trachea. In *Boorman's Pathology of the Rat*, 2nd ed.; Suttie, A., Ed.; Academic Press: Cambridge, MA, USA; Elsevier: London, UK, 2018.
49. Herbert, R.A.; Janardhan, K.S.; Pandiri, A.R.; Cesta, M.F.; Chen, V.; Miller, R.A. Lung, pleura, and mediastinum. In *Boorman's Pathology of the Rat*, 2nd ed.; Suttie, A., Ed.; Academic Press: Cambridge, MA, USA; Elsevier: London, UK, 2018.
50. Suarez, C.J.; Dintzis, S.M.; Frevert, C.W. Respiratory. In *Comparative Anatomy and Histology a Mouse and Human Atlas*, 1st ed.; Treuting, P.M., Dintzis, S.M., Eds.; Academic Press: Cambridge, MA, USA; Elsevier: London, UK, 2012.

51. Chamanza, R.; Wright, J.A. A Review of the Comparative Anatomy, Histology, Physiology and Pathology of the Nasal Cavity of Rats, Mice, Dogs and Non-human Primates. Relevance to Inhalation Toxicology and Human Health Risk Assessment. *J. Comp. Pathol.* **2015**, *153*, 287–314. [[CrossRef](#)]
52. Booth, W.D.; Baldwin, B.A.; Poynder, T.M.; Bannister, L.H.; Gower, D.B. Degeneration and regeneration of the olfactory epithelium after olfactory bulb ablation in the pig: A morphological and electrophysiological study. *Q. J. Exp. Physiol.* **1981**, *66*, 533–540. [[CrossRef](#)]
53. Lum, H.; Mitzner, W. A species comparison of alveolar size and surface forces. *J. Appl. Physiol.* **1987**, *62*, 1865–1871. [[CrossRef](#)]
54. Ackerman, M. Respiratory Tract. In *Biology of the Domestic Pig*; Pond, W., Mersmann, H., Eds.; Cornell University Press: Ithaca, NY, USA, 2001; pp. 502–532.
55. Krejci, J.; Nechvatalova, K.; Blahutkova, M.; Faldyna, M. The respiratory tract in pigs and its immune system: A review. *Vet. Med.* **2013**, *58*, 206–220. [[CrossRef](#)]
56. Horowitz, L.F.; Saraiva, L.R.; Kuang, D.; Yoon, K.H.; Buck, L.B. Olfactory receptor patterning in a higher primate. *J. Neurosci.* **2014**, *34*, 12241–12252. [[CrossRef](#)]
57. Judge, E.P.; Hughes, J.M.; Egan, J.J.; Maguire, M.; Molloy, E.L.; O’Dea, S. Anatomy and bronchoscopy of the porcine lung. A model for translational respiratory medicine. *Am. J. Respir. Cell Mol. Biol.* **2014**, *51*, 334–343. [[CrossRef](#)]
58. Parent, R. *Comparative Biology of the Normal Lung*, 2nd ed.; Elsevier: London, UK, 2015.
59. Choi, R.; Goldstein, B.J. Olfactory epithelium: Cells, clinical disorders, and insights from an adult stem cell niche. *Laryngoscope Investig. Otolaryngol.* **2018**, *3*, 35–42. [[CrossRef](#)]
60. Jeffrey, A.M.; Iatropoulos, M.J.; Williams, G.M. Nasal cytotoxic and carcinogenic activities of systemically distributed organic chemicals. *Toxicol. Pathol.* **2006**, *34*, 827–852. [[CrossRef](#)] [[PubMed](#)]
61. Strocchi, P.; Dozza, B.; Pecorella, I.; Fresina, M.; Campos, E.; Stirpe, F. Lesions caused by ricin applied to rabbit eyes. *Investig. Ophthalmol. Vis. Sci.* **2005**, *46*, 1113–1116. [[CrossRef](#)] [[PubMed](#)]
62. ASKJPC Joint Pathology Center Systemic Pathology Respiratory System September 2017 P-T04. Available online: https://www.askjpc.org/vspo/show_page.php?id=aUtBWFpmVnh4S0NKbFNsN1d1bXMzUT09 (accessed on 23 February 2021).
63. Moore, B.B.; Hogaboam, C.M. Murine models of pulmonary fibrosis. *Am. J. Physiol. Lung Cell. Mol. Physiol.* **2008**, *294*, L152–L160. [[CrossRef](#)] [[PubMed](#)]
64. Moore, B.B.; Lawson, W.E.; Oury, T.D.; Sisson, T.H.; Raghavendran, K.; Hogaboam, C.M. Animal models of fibrotic lung disease. *Am. J. Respir. Cell Mol. Biol.* **2013**, *49*, 167–179. [[CrossRef](#)]
65. Heppleston, A.G.; Leopo Ld, J.G. Chronic pulmonary emphysema: Anatomy and pathogenesis. *Am. J. Med.* **1961**, *31*, 279–291. [[CrossRef](#)]
66. Van Slyke, G.; Sully, E.K.; Bohorova, N.; Bohorov, O.; Kim, D.; Pauly, M.H.; Whaley, K.J.; Zeitlin, L.; Mantis, N.J. Humanized Monoclonal Antibody That Passively Protects Mice against Systemic and Intranasal Ricin Toxin Challenge. *Clin. Vaccine Immunol.* **2016**, *23*, 795–799. [[CrossRef](#)]
67. Falach, R.; Sapoznikov, A.; Evgy, Y.; Aftalion, M.; Makovitzki, A.; Agami, A.; Mimran, A.; Lerer, E.; Ben David, A.; Zichel, R.; et al. Post-Exposure Anti-Ricin Treatment Protects Swine Against Lethal Systemic and Pulmonary Exposures. *Toxins* **2020**, *12*, 354. [[CrossRef](#)]
68. Falach, R.; Sapoznikov, A.; Alcalay, R.; Aftalion, M.; Ehrlich, S.; Makovitzki, A.; Agami, A.; Mimran, A.; Rosner, A.; Sabo, T.; et al. Generation of Highly Efficient Equine-Derived Antibodies for Post-Exposure Treatment of Ricin Intoxications by Vaccination with Monomerized Ricin. *Toxins* **2018**, *10*, 466. [[CrossRef](#)]
69. Pratt, T.S.; Pincus, S.H.; Hale, M.L.; Moreira, A.L.; Roy, C.J.; Tchou-Wong, K.M. Oropharyngeal aspiration of ricin as a lung challenge model for evaluation of the therapeutic index of antibodies against ricin A-chain for post-exposure treatment. *Exp. Lung Res.* **2007**, *33*, 459–481. [[CrossRef](#)]
70. Phalen, R.F.; Mendez, L.B. Dosimetry considerations for animal aerosol inhalation studies. *Biomarkers* **2009**, *14* (Suppl. 1), 63–66. [[CrossRef](#)] [[PubMed](#)]
71. Cheng, P.; Li, S.; Chen, H. Macrophages in Lung Injury, Repair, and Fibrosis. *Cells* **2021**, *10*, 436. [[CrossRef](#)] [[PubMed](#)]

Disclaimer/Publisher’s Note: The statements, opinions and data contained in all publications are solely those of the individual author(s) and contributor(s) and not of MDPI and/or the editor(s). MDPI and/or the editor(s) disclaim responsibility for any injury to people or property resulting from any ideas, methods, instructions or products referred to in the content.